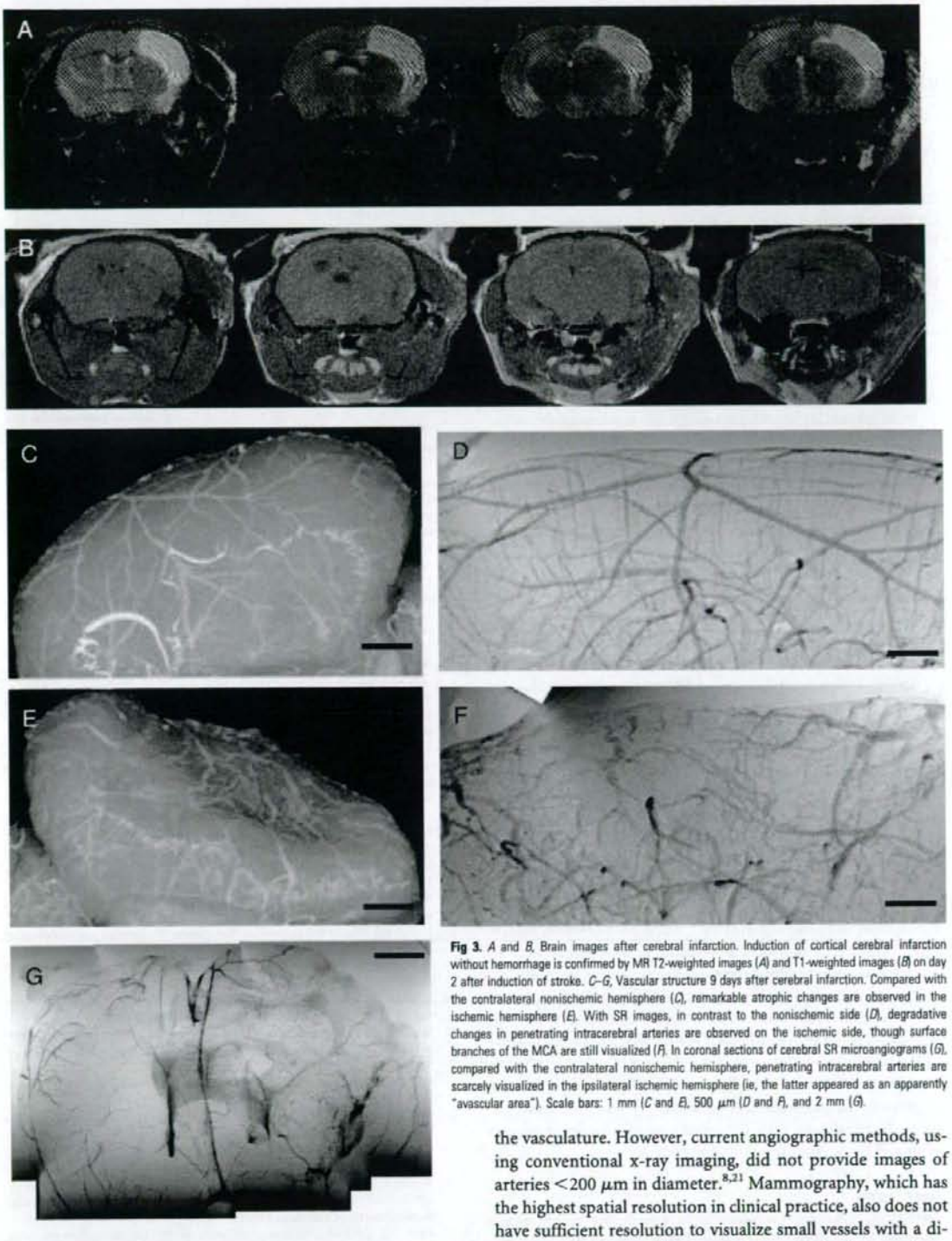

Fig 3. *A* and *B*, Brain images after cerebral infarction. Induction of cortical cerebral infarction without hemorrhage is confirmed by MR T2-weighted images (*A*) and T1-weighted images (*B*) on day 2 after induction of stroke. *C–G*, Vascular structure 9 days after cerebral infarction. Compared with the contralateral nonischemic hemisphere (*C*), remarkable atrophic changes are observed in the ischemic hemisphere (*E*). With SR images, in contrast to the nonischemic side (*D*), degradative changes in penetrating intracerebral arteries are observed on the ischemic side, though surface branches of the MCA are still visualized (*F*). In coronal sections of cerebral SR microangiograms (*G*), compared with the contralateral nonischemic hemisphere, penetrating intracerebral arteries are scarcely visualized in the ipsilateral ischemic hemisphere (ie, the latter appeared as an apparently "avascular area"). Scale bars: 1 mm (*C* and *E*), 500 μm (*D* and *F*), and 2 mm (*G*).

phology of small cerebral vessels in situ through imaging studies. Herein, we demonstrate that small cerebral vessels can be clearly visualized by microangiography by using SR.

Conventional angiography is commonly used to evaluate the vasculature. However, current angiographic methods, using conventional x-ray imaging, did not provide images of arteries <200 μm in diameter.[8,21] Mammography, which has the highest spatial resolution in clinical practice, also does not have sufficient resolution to visualize small vessels with a diameter of <50 μm.[11] Microangiographic techniques have been developed by using fine-focus x-rays and sensitive films to evaluate the microcirculation in the brain.[20] These methods enable visualization of human cortical perforating arteries and

medullary long branches (100 μm in diameter) by using 1-cm-thick sections of brain.[20] However, the limit of detection by using these methods applied to thick sections has been reported to be vessels of 50 μm in diameter.[22] Furthermore, visualization of smaller arteries required thin sections cut with a microtome.[20] The latter method is not well-suited to the evaluation of 3D cerebral vascular trees.

Compared with these conventional methods, the principal advantage of SR is the small size of the electron beam, thereby providing a high-intensity x-ray point source. Using a nearly parallel beam of SR, along with a precise detection system (pixel size of 4.5 μm), allowed us to obtain high-quality angiographic images with excellent spatial resolution. Furthermore, setting SR at an energy level just above the K absorption of barium produced the highest contrast images. SR imaging provides a powerful tool to reveal the morphology of small cerebral arteries such as superficial and deep penetrating arteries, allowing analysis of their physiologic and pathologic properties under a variety of conditions (ie, borderzone in infarction[23,24] and microaneurysm formation).

Fluorescence microscopy is another tool potentially useful for analysis of the microcirculation.[25] Although fluorescence microscopy provides visualization of microcirculation at the brain surface, the advantage of SR imaging is visualization of small vessels that have penetrated into the brain parenchyma, such as the subcortex. In addition, SR imaging allows performance of microangiography with an optimal projection. When the latter is combined with a microinjector, sequential real-time images can be obtained, providing the substrate for hemodynamic analysis.

In this article, we investigated SR imaging after stroke and showed that the SR image reflects pathologic changes previously observed by using anatomic/microscopic analysis. On day 9 after MCA occlusion, arteries on the surface of the cerebrum were visualized by SR, though penetrating intracerebral arteries were not detected. Previous studies have shown that the integrity of the distal cortical artery is usually maintained after occlusion of the proximal artery and that collateral flow is established through expansion of previously existing and/or formation of new vascular channels.[25,26] Analysis with enhanced MR imaging has shown cerebral parenchymal enhancement in the stroke area by 1 week after cerebral infarction,[27] indicative of blood flow in the peri-ischemic area. In contrast, penetrating intracerebral arteries were dramatically decreased in number in the ischemic hemisphere, though cortical branches on the brain surface were maintained after MCA occlusion. It has previously been shown that microvasculature in the ischemic territory displays adhesion of polymorphonuclear leukocytes in postcapillary venules, followed by the disruption of the microvascular network.[28] These previous findings are consistent with the results of our vascular images obtained by SR after ligation of the MCA.

Conclusion

Our study demonstrates, for the first time, the morphologic features of small vascular networks in murine brain by microangiography by using SR imaging. Our approach provides a powerful tool for evaluating potential angiogenic/antiangiogenic therapeutic strategies, as well as pathologic examination of the cerebral microarterial tree.

Acknowledgments

We thank Y. Kasahara, K. Tomiyasu, and M. Aoki for technical assistance.

References

1. Phillips SJ, Whisnant JP. **Hypertension and the brain: The National High Blood Pressure Education Program.** *Arch Intern Med* 1992;152:938–45
2. Ito K, Tanaka E, Mori H, et al. **A microangiographic technique using synchrotron radiation to visualize dermal circulation in vivo.** *Plast Reconstr Surg* 1998;102:1128–33
3. Tokiya R, Umetani K, Imai S, et al. **Observation of microvasculatures in athymic nude rat transplanted tumor using synchrotron radiation microangiography system.** *Academic Radiology* 2004;9:1039–46
4. Takeshita S, Isshiki T, Mori H, et al. **Use of synchrotron radiation microangiography to assess development of small collateral arteries in a rat model of hindlimb ischemia.** *Circulation* 1997;95:805–08
5. Conway JG, Popp JA, Thurman RG. **Microcirculation in periportal and pericentral regions of lobule in perfused rat liver.** *Am J Physiol* 1985;249:G449–56
6. Stock RJ, Cilento EV, McCuskey RS. **A quantitative study of fluorescein isothiocyanate-dextran transport in the microcirculation of the isolated perfused rat liver.** *Hepatology* 1989;9:75–82
7. Birngruber R, Schmidt-Erfurth U, Teschner S, et al. **Confocal laser scanning fluorescence topography: a new method for three-dimensional functional imaging of vascular structures.** *Graefes Arch Clin Exp Ophthalmol* 2000;238:559–65
8. Mori H, Hyodo K, Tanaka E, et al. **Small-vessel radiography in situ with monochromatic synchrotron radiation.** *Radiology* 1996;201:173–77
9. Umetani K, Yagi N, Suzuki Y, et al. **Observation and analysis of microcirculation using high-spatial-resolution image detectors and synchrotron radiation.** *Proceeding of SPIE* 2000;3977:522–33
10. Yamashita T, Kawashima S, Ozaki M, et al. **Images in cardiovascular medicine: mouse coronary angiograph using synchrotron radiation microangiography.** *Circulation* 2002;105:E3–4
11. Kuzmiak CM, Pisano ED, Cole EB, et al. **Comparison of full-field digital mammography to screen-film mammography with respect to contrast and spatial resolution in tissue equivalent breast phantoms.** *Med Phys* 2005;32:3144–50
12. Taguchi A, Soma T, Tanaka H, et al. **Administration of CD34+ cells after stroke enhances neurogenesis via angiogenesis in a mouse model.** *J Clin Invest* 2004;114:330–38
13. Furuya K, Kawahara N, Kawai K, et al. **Proximal occlusion of the middle cerebral artery in C57Black6 mice: relationship of patency of the posterior communicating artery, infarct evolution, and animal survival.** *J Neurosurg* 2004;100:97–105
14. Kitagawa K, Matsumoto M, Mabuchi T, et al. **Deficiency of intercellular adhesion molecule 1 attenuates microcirculatory disturbance and infarction size in focal cerebral ischemia.** *J Cereb Blood Flow Metab* 1998;18:1336–45
15. Matsushita K, Matsuyama T, Nishimura H, et al. **Marked, sustained expression of a novel 150-kDa oxygen-regulated stress protein, in severely ischemic mouse neurons.** *Brain Res Mol Brain Res* 1998;60:98–106
16. Coyne EF, Ngai AC, Meno JR, et al. **Methods for isolation and characterization of intracerebral arterioles in the C57/BL6 wild-type mouse.** *J Neurosci Methods* 2002;120:145–53
17. Herman LH, Ostrowski AZ, Gurdjian ES. **Perforating branches of the middle cerebral artery: an anatomical study.** *Arch Neurol* 1963;8:32–34
18. Kaplan HA. **The lateral perforating branches of the anterior and middle cerebral arteries.** *J Neurosurg* 1965;23:305–10
19. de Reuck J. **The area of the deep perforating branches of the median cerebral artery in man** [in French]. *Acta Anat (Basel)* 1969;74:30–35
20. Salamon G, Combalbert A, Faure J, et al. **Microradiographic study of the arterial circulation of the brain.** *Prog Brain Res* 1968;30:33–41
21. Mori H, Hyodo K, Tobita K, et al. **Visualization of penetrating transmural arteries in situ by monochromatic synchrotron radiation.** *Circulation* 1994;89:863–71
22. Salamon G, Raybaud C, Michotey P, et al. **Angiographic study of cerebral convolutions and their area of vascularization** [in French]. *Rev Neurol (Paris)* 1975;131:259–84
23. Bogousslavsky J, Regli F. **Centrum ovale infarcts: subcortical infarction in the superficial territory of the middle cerebral artery.** *Neurology* 1992;42:1992–98
24. Donnan GA, Norrving B, Bamford JM, et al. **Subcortical infarctions: classification and terminology.** *Cerebrovasc Dis* 1993;3:248–51
25. Tomita Y, Kubis N, Calando Y, et al. **Long-term in vivo investigation of mouse cerebral microcirculation by fluorescence confocal microscopy in the area of focal ischemia.** *J Cereb Blood Flow Metab* 2005;25:858–67
26. Zulch KJ. *Cerebral Circulation and Stroke.* Berlin, Germany: Springer-Verlag; 1971:116
27. Merten CL, Knitelius HO, Assheuer J, et al. **MRI of acute cerebral infarcts: increased contrast enhancement with continuous infusion of gadolinium.** *Neuroradiology* 1999;41:242–48
28. del Zoppo GJ, Mabuchi T. **Cerebral microvessel responses to focal ischemia.** *J Cereb Blood Flow Metab* 2003;23:879–94

Original Paper

European Neurology

Eur Neurol 2008;59:38–43
DOI: 10.1159/000109259

Received: October 4, 2006
Accepted: April 11, 2007
Published online: October 4, 2007

Relationship between Detectability of Ischemic Lesions by Diffusion-Weighted Imaging and Embolic Sources in Transient Ischemic Attacks

Hisakazu Uno[a] Akihiko Taguchi[a] Hiroshi Oe[a] Keiko Nagano[a]
Naoaki Yamada[b] Hiroshi Moriwaki[a] Hiroaki Naritomi[a]

Departments of [a]Cerebrovascular Medicine and [b]Radiology, National Cardiovascular Center, Suita, Japan

Key Words
Diffusion-weighted imaging · Embolic sources · Transient ischemic attacks

Abstract
Background/Aims: The aim of this study is to clarify the relationship between lesion detectability by diffusion-weighted magnetic resonance imaging (DWI) and the etiology of transient ischemic attacks (TIAs). ***Methods:*** A retrospective study was performed on 72 patients with carotid TIAs who underwent DWI studies within 2 weeks after the last episode. ***Results:*** Lesions were detected in 24 of 72 patients (33%). The detectability of lesions was 12% (3/25) in the large-artery atherosclerosis (LA) group, 57% (8/14) in the cardioembolism (CE) group, 8% (1/13) in the small-artery occlusion (SA) group, and 60% (12/20) in the other etiology or undetermined etiology (UD) group. Detectabilities in the CE group and the UD group were higher than those in the LA and SA groups. Of 24 patients with DWI-positive lesions, 17 (71%) had embolic sources in the heart; 9 were classified in the UD group because they had embolic sources both in the heart and large artery. ***Conclusion:*** Ischemic DWI lesions in TIAs are most likely caused by a cardioembolic mechanism. In TIA patients showing lesions on DWI, heart disease should be surveyed as the possible embolic source.

Introduction

According to the Ad Hoc Committee on classification of cerebrovascular disease of 1975, transient ischemic attacks (TIAs) are defined as ischemic cerebrovascular disease in which focal cerebral dysfunction resolves within 24 h [1]. It has been known for years that CT or T_1- and T_2-weighted magnetic resonance imaging (MRI) may occasionally depict small ischemic lesions in TIA patients [2–7]. More recently, diffusion-weighted imaging (DWI) has made it possible to demonstrate ischemic lesions in TIA patients with relatively high frequency [8]. Several studies have shown that the detectability of DWI lesions in TIA patients increases in correlation with the duration of TIA symptoms. However, clarification as to whether the detectability of DWI lesions is related to the etiology of TIA is still lacking. In the majority of previous studies reporting DWI detectability of TIA lesions, both types of TIAs – in the carotid artery territory and the vertebral artery territory – were included indiscriminately. This makes accurate evaluation of TIA duration difficult, since onset and end of symptoms are often obscure in a vertebral artery territory TIA. Therefore, we included only patients with carotid TIA in the present study, examining the relationship between the etiology of TIA and the detectability of DWI lesions.

KARGER

Fax +41 61 306 12 34
E-Mail karger@karger.ch
www.karger.com

0014–3022/08/0592–0038$24.50/0

Accessible online at:
www.karger.com/ene

Hiroaki Naritomi
Department of Cerebrovascular Medicine
National Cardiovascular Center
5-7-1 Fujishiro-dai, Suita 565-8565 (Japan)
Tel. +81 6 6833 5012, Fax +81 6 6835 5137, E-Mail hnaritom@hsp.ncvc.go.jp

Subjects and Methods

A retrospective analysis was performed on 72 patients with carotid TIA who were admitted to our department during the interval from May 1998 to July 2005, and who underwent DWI studies within 14 days of symptom onset after the last TIA. Fifty-two patients were male. The mean (± SD) age of patients was 69 ± 10 years. Patients with isolated amaurosis fugax were excluded. MRI was performed using a Siemens Magnetom Vision 1.5-tesla MR unit. DWI scanning was performed with a single-shot, multislice spin echo and echo planar imaging sequence. DWI parameters comprised: TE = 123 ms; FOV = 23 × 23 cm; matrix = 128 × 200, and slice thickness = 4 mm. Diffusion gradients were applied in the through-plane direction with a b value of 1,100 s/mm^2. Since 1999, imaging parameters have been changed to TE = 100 ms and matrix = 98 × 128. Diffusion gradients were applied in each x, y, and z direction with b values of 1,000 s/mm^2, and trace imaging was calculated. Conventional MRI studies included T_1-weighted (TR/TE: 630/14) and T_2-weighted (TR/TE: 5,400/99) images, and fluid attenuation inversion recovery (TR/TE/TE: 9,000/105/2,400) images were obtained when required.

We assessed whether each patient had ischemic lesions and/or arterial disease compatible with symptoms by reviewing DWI films and the results of conventional cerebral angiography, MR angiography, and carotid ultrasonography. We assessed the presence or absence of cardiac embolic sources based on 12-lead ECG findings, transthoracic and/or transesophageal echocardiography and, when required, 24-hour ECG monitoring. Referring to the TOAST classification [9], all patients were classified into four groups: large-artery atherosclerosis (LA) group, cardioembolism (CE) group, small-artery occlusion (SA) group, and other etiology or undetermined etiology (UD) group. The LA group included patients with more than 50% stenosis of intracranial or extracranial large arteries or with a complicated lesion of more than 3.5 mm in the aortic arch based on findings of conventional cerebral angiography, MR angiography, carotid ultrasonography and transesophageal echocardiography. Patients in this group should not have had significant heart disease. The CE group included patients with significant heart disease that can become an embolic source, such as mechanical prosthetic valves, mitral stenosis with atrial fibrillation, atrial fibrillation, left atrial/atrial appendage thrombus, sick sinus syndrome, recent myocardial infarction within 4 weeks prior to the study, left ventricular thrombus, dilated cardiomyopathy, akinetic left ventricular segment, atrial myxoma, infective endocarditis or patent foramen ovale with peripheral thrombus but without LA. The SA group included patients who had neither significant heart disease nor LA, nor other evidence of disease. The TIA symptoms in this group should have corresponded to any of the traditional clinical lacunar syndromes and should not have been associated with cortical symptoms. The UD group included patients who could not have been classified into other groups because of the following reasons: (1) they had other causes of cerebral ischemia, such as dissection of cervical/cranial arteries, vasculitis or hypercoagulopathy, (2) they had cortical symptoms in spite of an absence of association with significant heart disease, large-artery lesions or evidence of other diseases, and (3) they had both significant heart disease and more than 50% stenosis in a large artery or aortic complicated lesions greater than 3.5 mm. This classification was made by mutual agreement by three neurologists. We also examined the duration of TIA symptoms and the time from onset of TIA to DWI in each patient. Furthermore, we reviewed the correlation between these factors and the detectability of lesions. We also studied whether patients had risk factors for atherosclerosis such as hypertension, diabetes mellitus, hyperlipidemia and smoking, and whether they had a history of cerebral infarction.

Statistical Analysis

Statistical analysis was performed using a commercially available software package (Statview, version 5, SAS Institute Inc., Cary, N.C., USA). Data were expressed as means ± SD. The level of $p < 0.05$ was determined to indicate statistical significance. We statistically compared the four groups as classified above using one-way factorial ANOVA or the Kruskal-Wallis test.

The table of baseline patient characteristics was analyzed using the Yates corrected χ^2 or Fisher test, as appropriate.

Results

Twenty-four of 72 patients (33%) had small ischemic lesions on DWI. There was no significant difference in baseline characteristics between patients with positive DWI lesions and those with negative DWI lesions (table 1). As shown in table 2, the duration of symptoms was significantly longer in patients with positive DWI lesions (4.0 ± 5.1 h) than in those with negative DWI lesions (1.4 ± 2.5 h) ($p < 0.01$). The time from TIA onset to DWI study was also significantly longer in patients with positive lesions (4.5 ± 4.1 days) than in those with negative lesions (2.0 ± 3.2 days) ($p < 0.01$). The detectability of lesions increased in correlation with the duration of TIA symptoms, as shown in figure 1. The detectability of lesions was also influenced by time from TIA onset to DWI, as follows: detectability was 14% (4/29) in the group undergoing DWI at 0–12 h after TIA, 33% (5/15) in the group undergoing DWI at 12–24 h after TIA, 43% (3/7) in the group undergoing DWI at 1–3 days after TIA, 60% (6/10) in the group undergoing DWI at 3–7 days after TIA, 57% (4/7) in the group undergoing DWI at 7–10 days after TIA, and 50% (2/4) in the group undergoing DWI at 10–14 days after TIA. Thus, the detectability of lesions was somewhat lower in patients undergoing DWI within 24 h after TIA than in those undergoing DWI more than 24 h after TIA.

Cerebral angiography was carried out on 25 patients, MR angiography on 58 patients, carotid ultrasonography on 71 patients, transthoracic echocardiography on 58 patients and transesophageal echocardiography on 60 patients. The type of etiology was classified as LA group, 25 patients; CE group, 14 patients; SA group, 13 patients, and UD group, 20 patients. The breakdown of the 20 patients

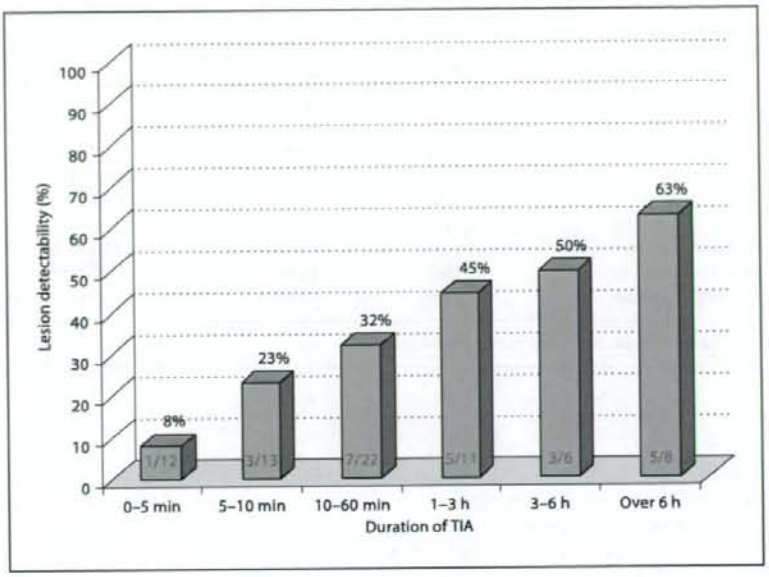

Fig. 1. The duration of TIA symptoms and DWI lesion detectability. The DWI lesion detectability increases in correlation with the duration of TIA symptoms.

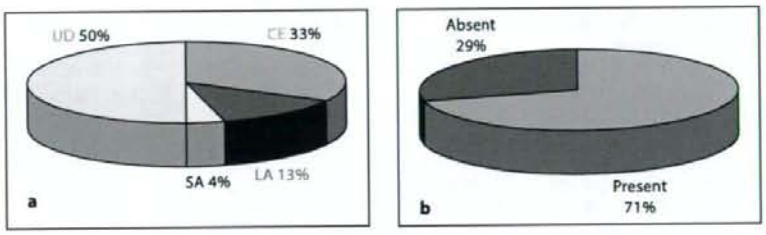

Fig. 2. Details of 24 TIA patients with DWI-positive lesions. **a** 83% of DWI-positive patients belong to the CE or UD groups. **b** 71% of DWI-positive patients have heart disease, either independently or in association with other etiologies.

in the UD group was as follows: (1) 1 patient with both antiphospholipid antibody syndrome and a significant lesion in a large artery, and 1 other patient with cervicocranial dissection and significant atherosclerotic lesions in a large artery, (2) 2 patients with cortical symptoms in association with no abnormality in the heart, large artery and other tests, and (3) 16 patients with both significant heart disease and significant stenotic lesions in large cerebral arteries and/or aorta. As shown in table 3, the detectabilities of lesions in the CE group (57%) and the UD group (60%) were significantly higher as compared with those in the LA group (12%) and the SA group (8%).

The duration of symptoms in the CE group was somewhat longer than in the other three groups, although the difference was not significant (table 3). Time from TIA onset to DWI was somewhat longer in the CE and UD groups as compared with the other two groups. However, results of one-way factorial ANOVA indicated that there was no significant difference in time from TIA to DWI studies between the groups (table 3). DWI studies were performed within 24 h after TIA in 39 patients and more than 24 h after TIA in 33 patients. Percentages of patients undergoing DWI studies within 24 h after TIA were 64% (16/25) in the LA group, 50% (7/14) in the CE group, 62% (8/13) in the SA group, and 40% (8/20) in the UD group. There were no significant differences in the frequency of early DWI studies between the four groups (Kruskal-Wallis test). The CE and UD groups had higher lesion detectability irrespective of time from TIA to DWI studies.

A total of 14 patients had multiple lesions on DWI. The frequency of multiple lesions in each group was as fol-

Table 1. Baseline patient characteristics

	DWI positive (n = 24)	DWI negative (n = 48)
Age, years	68 ± 10	69 ± 10
Male gender	18 (75)	34 (71)
Hypertension	15 (63)	34 (71)
Diabetes mellitus	4 (17)	10 (21)
Hypercholesterolemia	9 (38)	21 (44)
Smoking	13 (54)	31 (65)
History of stroke	1 (4)	8 (17)

Figures in parentheses indicate percentages.

Table 2. Duration of symptoms and time to MRI studies in DWI-positive and DWI-negative patients

	DWI positive	DWI negative
Duration of symptoms, h	4.0 ± 5.1*	1.4 ± 2.5
Time from TIA to MRI, days	4.5 ± 4.1*	2.0 ± 3.2

* $p < 0.01$: significantly longer as compared with the diffusion-negative patients.

Table 3. Comparison of four TIA groups

	LA (n = 25)	CE (n = 14)	SA (n = 13)	UD (n = 20)
Positive DWI lesions	3 (12)	8 (57)[1]	1 (8)	12 (60)[1]
Duration of symptoms, h	1.5 ± 3.0	3.8 ± 5.2	1.7 ± 2.8	2.5 ± 3.9
Time from TIA to DWI, days	1.8 ± 2.6	3.6 ± 4.1	2.6 ± 4.5	3.6 ± 4.1

Figures in parentheses indicate percentages.
[1] The frequency of DWI-positive lesions is significantly higher in the CE and the UD groups as compared with the LA and SA groups ($p < 0.05$).

Table 4. The type of heart diseases and lesion detectability in the CE group

Type of heart diseases	DWI positive	DWI negative
Atrial fibrillation	5	2
Mechanical prosthetic valve	1	1
Akinetic left ventricular segment	2	0
Sick sinus syndrome	0	1
Patent foramen ovale with peripheral thrombus	0	2

lows: in the LA group, 2 of 3 patients with positive lesions (67%) had multiple lesions; the number of lesions was 3 and 5, respectively. In the CE group, 3 of 8 patients (38%) had multiple lesions; the number of lesions was 3 in 2 cases and 4 in the other. In the SA group, 1 positive patient had only a single lesion (0%). In the UD group, 9 of 12 patients (75%) had multiple lesions; the number of lesions was 2 in 5 cases, 3 in 3 cases and 6 in the remainder. Thus, no remarkable relationship was observed between the number of lesions and the etiology.

Of all 24 patients with ischemic lesions on DWI, 8 patients (33%) belonged to the CE group, 12 patients (50%) to the UD group, 3 patients (13%) to the LA group, and 1 patient (4%) to the SA group (fig. 2). Of the 12 patients with positive DWI lesions who belonged to the UD group, 9 had significant heart disease in association with significant large-artery lesions. Thus, of all 24 patients with ischemic lesions on DWI, 17 patients (71%) had significant heart disease either independently or concomitantly with large-artery lesions (fig. 2). In the CE group, 5 of 7 patients with atrial fibrillation had positive DWI lesions (table 4).

Discussion

In recent years, quite a few studies have reported the presence of ischemic lesions on DWI following TIA. In these previous studies, the detectability of TIA lesions on DWI ranged from 20 to 70% [8, 10–16]. Detectability in the present study was 33%, showing a somewhat lower value as compared with previous studies. This may be partly related to the difference in the timing of DWI examinations between the present study and the previous studies. In the present study, approximately 54% of patients underwent DWI within 24 h after TIA onset; the detectability in these patients was low, at 21%. On the other hand, in most previous studies the majority of TIA patients underwent DWI examinations more than 24 h after TIA onset. When we calculated only the detectability of lesions in our patients undergoing DWI more than 24 h after TIA onset, the detectability increased to 48%, showing similar values to those reported in previous studies. The above-mentioned reasoning can also be inferred from the study of Rovira et al. [10]. In their study,

only 9% of patients underwent DWI within 48 h after TIA, and the detectability of lesions in the entire group showed a high value, reaching 67%. In a transient ischemia experiment using rats, the value of the average apparent diffusion coefficient decreased significantly during the ischemic period and then normalized at 60–90 min after ischemia, followed again subsequently by a significant reduction more than 12 h after ischemia [17]. As confirmed in the above experiment, the detectability of lesions on DWI may decrease for a while after a short period of transient cerebral ischemia, and may increase thereafter, although the mechanisms remain unclear. Kidwell et al. [8] first pointed out that the detectability of lesions on DWI in patients with TIA increases in correlation with the duration of symptoms. Since then, similar results have been reported by several authors. In the study by Rovira et al. [10], the detectability of lesions in TIA patients with symptoms lasting less than 6 h was 59%, whereas the value was 100% in patients with symptoms lasting more than 6 h. Crisostomo et al. [11] reported that the detectability of lesions in patients with symptoms lasting more than 1 h was significantly higher as compared with patients with symptoms lasting less than 1 h. Inatomi et al. [12] also reported that the detectability of lesions was significantly higher in TIA patients with symptoms lasting more than 30 min than in those with symptoms lasting less than 30 min. In our study, the detectability of lesions also tended to increase according to the increase in TIA duration.

Previously, few workers performed detailed investigations on the relationship between the detectability of DWI lesions and the etiology of TIA. Rovira et al. [10] reported that the detectability of DWI lesions was higher in TIA patients with large-artery lesions than in those with cardiac lesions. However, the report lacks credibility, since the number of patients in their study was small; only 4 patients had cardiac lesions, whereas 19 patients had large-artery lesions. Nakamura et al. [16] reported higher detectability of DWI lesions in TIA patients with atrial fibrillation as compared with those without atrial fibrillation. However, they focused only on atrial fibrillation and did not clarify DWI detectability in TIA patients without atrial fibrillation who had other types of heart diseases. In the present study, the presence or absence of large-artery lesions and/or cardiac disease was surveyed in a retrospective manner reviewing the results of conventional cerebral angiography, MR angiography, carotid ultrasonography, 12-lead ECG, transthoracic or transesophageal echocardiography, and 24-hour ECG monitoring. The patients were then classified into four groups according to the etiology of TIA, such as LA, CE, SA and UD groups. The results indicated that the detectability of lesions in the CE group and the UD group was higher than that in the other groups. Time from TIA to DWI studies was almost the same in the four groups. Lesion detectability was higher in the CE and UD groups than in the other groups, even when the comparison among the subgroups undergoing DWI studies had been made within 24 h after TIA onset. Therefore, the higher detectability in the CE and UD groups is unrelated to time from TIA to DWI studies. The mean duration of TIA symptoms in the CE group was more than 3 h, which was the longest of all the groups. In general, cardioembolic stroke produces severer symptoms than artery-to-artery embolic stroke. This may be attributable to the fact that emboli originating in the heart tend to occlude larger blood vessels for longer durations as compared with artery-to-artery emboli. This is probably also true in cases of TIA. Microemboli originating in the heart likely occlude larger blood vessels for longer durations as compared with artery-to-artery microemboli. Accordingly, ischemic duration may be longer in TIA patients with heart disease than in those with other types of etiology, and ischemic lesions may be larger in TIA patients with heart disease than in those with other types of etiology. Probably for such reasons, ischemic lesions in cardioembolic TIA may be more readily found on DWI than those in other types of TIA. In the present study, 16 of 20 patients in the UD group had heart disease, and 9 had ischemic lesions on DWI. In these 9 patients, TIA was most likely caused by a cardioembolic mechanism rather than another type of etiology. Johnston et al. [18] conducted a follow-up study in 1,707 patients with TIA for 90 days. In their study, 10.5% of patients developed cardioembolic stroke during the follow-up period, and approximately half of them had stroke within 48 h after TIA. Thus, cardioembolic stroke may occur soon after TIA at a considerably high frequency. A DWI study is considered useful to evaluate etiological mechanisms of TIA. If ischemic lesions are detected on DWI, the presence of heart disease should be suspected, and appropriate medication should be considered to prevent cardioembolic stroke.

Acknowledgement

This work was supported by a Research Grant for Cardiovascular Diseases (18C-2) funded by the Japanese Ministry of Health and Labor.

References

1 Ad Hoc Committee on Cerebrovascular Disease: A classification and outline of cerebrovascular disease. Part 2. Stroke 1975;6:564–616.

2 Ladurner G, Sager WD, Iliff LD, Lechner H: A correlation of clinical findings and CT in ischemic cerebrovascular disease. Eur Neurol 1979;18:281–288.

3 Dávalos A, Matías-Guiu J, Torrent O, Vilaseca J, Codina A: Computed tomography in reversible ischaemic attacks: clinical and prognostic correlations in a prospective study. J Neurol 1988;235:155–158.

4 Calandre L, Gomara S, Bermejo F, Millan JM, del Pozo G: Clinical-CT correlations in TIA, RIND, and strokes with minimum residuum. Stroke 1984;15:663–666.

5 Bogousslavsky J, Regli F: Cerebral infarct in apparent transient attack. Neurology 1985; 35:1501–1503.

6 Perrone P, Candelise L, Scotti G, De Grandi C, Scialfa G: CT evaluation in patients with transient ischemic attack. Correlation between clinical and angiographic findings. Eur Neurol 1979;18:217–221.

7 Fazekas F, Fazekas G, Schmidt R, Kapeller P, Offenbacher H: Magnetic resonance imaging correlates of transient cerebral ischemic attacks. Stroke 1996;27:607–611.

8 Kidwell CS, Alger JR, Di Salle F, Starkman S: Diffusion MRI in patients with transient ischemic attacks. Stroke 1999;30:1174–1180.

9 Adams HP Jr, Bendixen BH, Kappele LJ, Biller J, Love BB, Gordon DL, Marsh EE; the TOAST Investigators: Classification of subtype of acute ischemic stroke: definition for use in a multicenter clinical trial. Stroke 1993;24:35–41.

10 Rovira A, Rovira-Gols A, Pedraza S, Grivé E, Molina C, Alvarez-Sabín J: Diffusion-weighted MR imaging in the acute phase of transient ischemic attacks. AJNR Am J Neuroradiol 2002;23:77–83.

11 Crisostomo RA, Garcia MM, Tong DC: Detection of diffusion-weighted MRI abnormalities in patients with transient ischemic attack. Correlation with clinical characteristics. Stroke 2003;34:932–937.

12 Inatomi Y, Kimura K, Yonehara T, Fujioka S, Uchino M: DWI abnormalities and clinical characteristics in TIA patients. Neurology 2004;62:376–380.

13 Takayama H, Mihara B, Kobayashi M, Hozumi A, Sadanaga H, Gomi S: Usefulness of diffusion-weighted MRI in the diagnosis of transient ischemic attacks (in Japanese). No To Shinkei 2000;52:919–923.

14 Engelter ST, Provenzale JM, Petrella JR, Alberts MJ: Diffusion MRI imaging and transient ischemic attacks. Stroke 1999;30:2762–2763.

15 Bisschops RHC, Kappelle LJ, Mali WPTM, van der Grond J: Hemodynamic and metabolic changes in transient ischemic attack patients. A magnetic resonance angiography and ^{1}H-magnetic resonance spectroscopy study performed within 3 days of onset of a transient ischemic attack. Stroke 2002;33: 110–115.

16 Nakamura T, Uchiyama S, Shibagaki Y, Iwata M: Abnormalities on diffusion-weighted magnetic resonance imaging in patients with transient ischemic attack. Clin Neurol 2003;43:122–125.

17 Li F, Silva MD, Sotak CH, Fisher M: Temporal evolution of ischemic injury evaluated with diffusion-, perfusion-, and T_2-weighted MRI. Neurology 2000;54:689–696.

18 Johnston SC, Gress DR, Browner WS, Sidney S: Short-term prognosis after emergency department diagnosis of TIA. JAMA 2000;284: 2901–2906.

Journal of Cerebral Blood Flow & Metabolism (2008) 28, 1086–1089

www.jcbfm.com

Brief Communication

Increase in circulating CD34-positive cells in patients with angiographic evidence of moyamoya-like vessels

Tomoyuki Yoshihara[1], Akihiko Taguchi[1], Tomohiro Matsuyama[2], Yoko Shimizu[1], Akie Kikuchi-Taura[3], Toshihiro Soma[3], David M Stern[4], Hiroo Yoshikawa[5], Yukiko Kasahara[1], Hiroshi Moriwaki[1], Kazuyuki Nagatsuka[1] and Hiroaki Naritomi[1]

[1]*Department of Cerebrovascular Disease, National Cardiovascular Center, Osaka, Japan;* [2]*Institute for Advanced Medical Sciences, Hyogo College of Medicine, Hyogo, Japan;* [3]*Department of Hematology, Osaka Minami National Medical Center, Osaka, Japan;* [4]*Dean's Office, College of Medicine, University of Cincinnati, Cincinnati, Ohio, USA;* [5]*Department of Internal Medicine, Hyogo College of Medicine, Hyogo, Japan*

Increasing evidence points to a role for circulating endothelial progenitor cells, including populations of CD34-positive (CD34$^+$) cells, in maintenance of cerebral blood flow. In this study, we investigated the link between the level of circulating CD34$^+$ cells and neovascularization at ischemic brain. Compared with control subjects, a remarkable increase of circulating CD34$^+$ cells was observed in patients with angiographic moyamoya vessels, although no significant change was observed in patients with major cerebral artery occlusion (or severe stenosis) but without moyamoya vessels. Our results suggest that the increased level of CD34$^+$ cells associated with ischemic stress is correlated with neovascularization at human ischemic brain.
Journal of Cerebral Blood Flow & Metabolism (2008) **28**, 1086–1089; doi:10.1038/jcbfm.2008.1; published online 30 January 2008

Keywords: antigens; CD34; moyamoya vessel; neovascularization

Introduction

Increasing evidence points to a role for bone marrow-derived immature cells, such as endothelial progenitor cells, in maintenance of vascular homeostasis and repair. CD34-positive (CD34$^+$) cells comprise a population enriched for endothelial progenitor cells whose contribution to neovasculature includes both direct participation in forming the neovessel and regulatory roles as sources of growth/angiogenesis factors (Majka *et al*, 2001). Previously, we have shown accelerated neovascularization after administration of CD34$^+$ cells in an experimental model of stroke (Taguchi *et al*, 2004*b*) and induced by autologous bone marrow mononuclear cells (rich cell fraction of CD34$^+$ cells) transplanted locally into patients with limb ischemia (Taguchi *et al*, 2003). In addition, we have observed a positive correlation between the level of circulating CD34$^+$ cells and regional blood flow (Taguchi *et al*, 2004*a*), and cognitive function (Taguchi *et al*, 2007) in patients with chronic cerebral ischemia.

In this study, we have evaluated the level of circulating CD34$^+$ cells in patients with unusually accelerated neovascularization induced by progressive occlusion (or severe stenosis) of the supraclinoid portion of the internal carotid artery, the proximal region of the anterior, and/or middle cerebral artery characterized angiographically by the presence of moyamoya-like vessels (Natori *et al*, 1997) that supply ischemic brain as collaterals. We have investigated the hypothesis that circulating bone marrow-derived immature cells might be associated with neovascularization at ischemic sites in the human brain.

Patients and methods

The institutional review board of the National Cardiovascular Center approved this study. All subjects provided

Correspondence: Dr A Taguchi, Department of Cerebrovascular Disease, National Cardiovascular Center, 5-7-1 Fujishiro-dai, Suita, Osaka 565-8565, Japan.
E-mail: taguchi@ri.ncvc.go.jp
This work was supported by a Grant-in-Aid for Scientific Research from the Ministry of Health, Labour, and Welfare (H19-Choujyu-029).
Received 29 October 2007; revised 19 December 2007; accepted 26 December 2007; published online 30 January 2008

informed consent. A total of 50 individuals, including 24 patients with occlusion or severe stenosis (>90%) at the C1 portion of the internal carotid artery or the M1 portion of the middle cerebral artery, and 26 age-matched healthy volunteers with cardiovascular risk factors, but without history of vascular disease, were enrolled. The diagnosis of cerebral artery occlusion or stenosis was made angiographically and four patients were found to have classical angiographic evidence of moyamoya-like vessels, including one with right C1 occlusion, one with right M1 occlusion, and two with bilateral C1 severe stenosis. All patients with cerebral artery occlusion or stenosis had a history of cerebral infarction. Individuals excluded from the study included patients who experienced a vascular event within 30 days of measurements, premenopausal women, and those with evidence of infection and/or malignant disease. The number of circulating CD34+ cells was quantified as described (Taguchi *et al*, 2007). In brief, blood samples (200 μl) were incubated with phycoerythrin-labeled anti-CD34 antibody, fluorescein isothiocyanate-labeled anti-CD45 antibody, 7-aminoactinomycin-D (7-AAD), and internal control (all of these reagents are in the Stem-Kit; BeckmanCoulter, Marseille, France). After incubation, samples were centrifuged, and supernatant was removed to obtain concentrated cell suspensions. 7-Aminoactinomycin-D-positive dead cells and CD45-negative cells were excluded, and the number of cells forming clusters characteristic of CD34+ cells (i.e., low side scatter and low-to-intermediate CD45 staining) was counted. The absolute number of CD34+ cells was calculated using the internal control. Mean cell number of duplicate measurements was used for quantitative analysis. Statistical comparisons among groups were determined using analysis of variance or χ^2 test. Individual comparisons were performed using a two-tailed unpaired Students' *t*-test or Mann–Whitney's *U*-test. Mean ± s.e. is shown.

Results

Enrolled individuals were divided into three groups: control subjects, patients with cerebral occlusion or severe stenosis, but without the presence of vessels with angiographic characteristics of moyamoya disease, and patients with angiographic evidence of moyamoya-like vessels. Baseline characteristics of the groups are shown in Table 1. The modified Rankin scale evaluation of patients with and without moyamoya-like vessels was 0.5 ± 0.5 and 1.3 ± 0.2, respectively ($P = 0.15$). Comparing these groups, there was a significant difference in the ratio of gender and treatment with aspirin between groups. However, no significant difference was observed in the number of circulating CD34+ cells in control group between genders (male, $n = 13$, CD34+ cells = $0.93 \pm 0.10/\mu$L; female, $n = 13$, CD34+ cells = $0.85 \pm 0.11/\mu$L; $P = 0.59$) and treatment with aspirin (aspirin (+), $n = 6$, CD34+ cells = $0.76 \pm 0.12/\mu$L; aspirin (−), $n = 20$, CD34+ cells = $0.93 \pm 0.09/\mu$L; $P = 0.26$), indicating mild and nonsignificant effects of gender and treatment with aspirin on the level of circulating CD34+ cells. In univariate analysis of control subjects, each cerebrovascular risk factor and treatment with statins showed no significant difference in the number of circulating CD34+ cells (data not shown).

A representative angiogram showing characteristics of moyamoya-like vessels is shown in Figures 1A and 1B. Angiographic moyamoya-like vessels were observed around the M1 portion of an occluded middle cerebral artery. Compared with a normal subject (Figure 1C) and patients without angiographic evidence of moyamoya-like vessels (Figure 1D), a remarkable increase in levels of

Table 1 Baseline characteristics

	Total	*Control*	*Major artery occlusion/stenosis*		P-*value for trend*
			Moyamoya (−)	*Moyamoya (+)*	
N	50	26	20	4	
Age, years	60.8 ± 1.1	60.5 ± 1.9	61.5 ± 1.0	59.3 ± 5.9	0.85
Male, *n* (%)	33 (66)	13 (50)	18 (90)	2 (50)	0.01
Risk factor, n (%)					
Hypertension	35 (70)	16 (62)	15 (75)	4 (100)	0.24
Hyperlipidemia	26 (52)	14 (54)	10 (50)	2 (50)	0.96
Diabetes mellitus	11 (22)	7 (27)	4 (20)	0 (0)	0.46
Smoking	15 (30)	7 (27)	8 (40)	0 (0)	0.25
Treatment, n (%)					
Ca channel blockers	20 (40)	10 (38)	8 (40)	2 (50)	0.91
β-Blockers	5 (10)	3 (11)	1 (5)	1 (25)	0.44
ACE inhibitor	7 (14)	4 (15)	2 (10)	1 (25)	0.70
ARB	12 (24)	5 (19)	5 (25)	2 (50)	0.40
Diuretics	4 (8)	2 (7)	1 (5)	1 (25)	0.40
Statin therapy	14 (28)	9 (34)	4 (20)	1 (25)	0.54
Aspirin	19 (38)	6 (23)	10 (50)	3 (75)	0.05
Ticlopidine	12 (24)	3 (11)	8 (40)	1 (25)	0.08

Abbreviations: ACE, angiotensin-converting enzyme; ARB, angiotensin 2 receptor blocker.

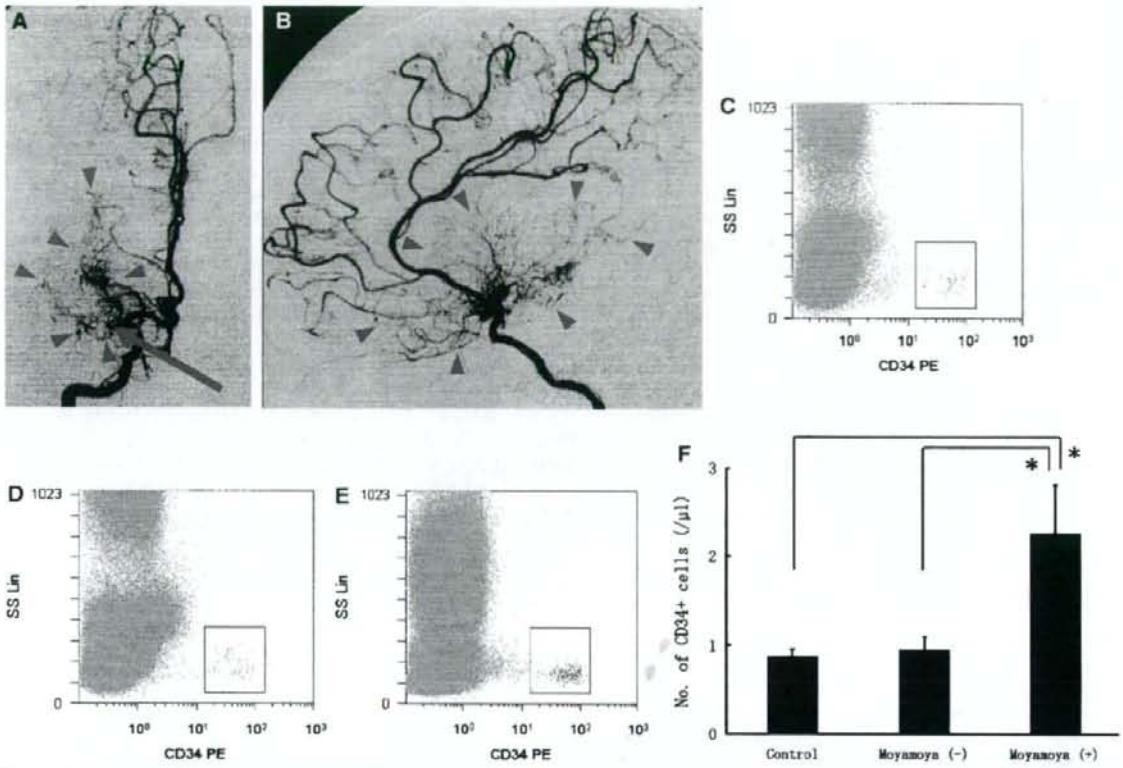

Figure 1 Increased levels of circulating CD34+ cells in patients with angiographic evidence of moyamoya-like vessels. (**A**, **B**) Representative angiogram from a patient with moyamoya-like vessels. Unusually accelerated neovascularization (based on angiographic features of moyamoya-like vessels, arrowheads) was observed around an occlusive M1 lesion (arrow). Anterior–posterior view (**A**) and lateral view (**B**) of the right internal carotid artery showed angiographically. (**C**–**E**) After exclusion of 7-aminoactinomycin-D (7-AAD)-positive dead cells and CD45-negative cells (nonleukocytes), CD34+ cells cluster at low side scatter. Representative fluorescence-activated cell sorting analyses from a control subject (**C**), a patient without moyamoya-like vessels (**D**), and a patient with moyamoya-like vessels (**E**) are shown. (**F**) A more than two-fold increase in circulating CD34+ cells was observed in patients with moyamoya-like vessels, compared with control subjects and patients without moyamoya-like vessels (*$P < 0.001$). SS Lin: side-scatter linear scale.

peripheral CD34+ cells was observed in patients with moyamoya-like vessels (Figure 1E) based on fluorescence-activated cell sorting. To confirm this impression, levels of circulating CD34+ cells were quantified (control, CD34+ cells = $0.89 \pm 0.07/\mu L$; moyamoya (−), CD34+ cells = $0.98 \pm 0.13/\mu L$; moyamoya (+), CD34+ cells = $2.28 \pm 0.53/\mu L$) and found to be significantly increased in patients with moyamoya-like vessels more than two-fold higher than in controls (Figure 1F, $P < 0.001$).

Discussion

In this study, we have found that a feature of unusually accelerated neovascularization, evidence of moyamoya-like vessels in the immediate locale of an occluded major cerebral artery, can be correlated with a robust increase in the level of circulating CD34+ cells. The latter was determined using a newly developed method that enables quantification of few CD34+ cells in peripheral blood in a highly reproducible manner.

After acute cerebral ischemia, mobilization of CD34+ cells from bone marrow has been shown in stroke patients (Taguchi *et al*, 2004*a*). Furthermore, transplantation of CD34+ cells (Taguchi *et al*, 2004*b*) and bone marrow cells (Borlongan *et al*, 2004*a*, *b*) has been shown to restore cerebral blood flow in experimental models of stroke. In chronic ischemia, transplantation of CD34+ cells has also been shown to accelerate neovascularization, including formation of collateral vessels, in patients with chronic ischemic heart disease (Boyle *et al*, 2006) and limb ischemia (Kudo *et al*, 2003). In addition, there is a report regarding the correlation between inadequate coronary collateral development and reduced numbers of circulating endothelial progenitor cells in

patients with myocardial ischemia (Lambiase *et al*, 2004). In this study, we show, for the first time, a correlation between neovascularization of the cerebral arterial circulation and increased levels of circulating CD34+ cells. Our results support the hypothesis that circulating CD34+ cells potentially contribute to neovascularization at sites of ischemic brain injury.

Acknowledgements

We thank K Obata and Y Okinaka for technical assistance.

Conflict of interest

The authors state no conflict of interest.

References

Borlongan CV, Lind JG, Dillon-Carter O, Yu G, Hadman M, Cheng C, Carroll J, Hess DC (2004*a*) Bone marrow grafts restore cerebral blood flow and blood brain barrier in stroke rats. *Brain Res* 1010:108–16

Borlongan CV, Lind JG, Dillon-Carter O, Yu G, Hadman M, Cheng C, Carroll J, Hess DC (2004*b*) Intracerebral xenografts of mouse bone marrow cells in adult rats facilitate restoration of cerebral blood flow and blood–brain barrier. *Brain Res* 1009:26–33

Boyle AJ, Whitbourn R, Schlicht S, Krum H, Kocher A, Nandurkar H, Bergmann S, Daniell M, O'Day J, Skerrett D, Haylock D, Gilbert RE, Itescu S (2006) Intra-coronary high-dose CD34+ stem cells in patients with chronic ischemic heart disease: a 12-month follow-up. *Int J Cardiol* 109:21–7

Kudo FA, Nishibe T, Nishibe M, Yasuda K (2003) Autologous transplantation of peripheral blood endothelial progenitor cells (CD34+) for therapeutic angiogenesis in patients with critical limb ischemia. *Int Angiol* 22:344–8

Lambiase PD, Edwards RJ, Anthopoulos P, Rahman S, Meng YG, Bucknall CA, Redwood SR, Pearson JD, Marber MS (2004) Circulating humoral factors and endothelial progenitor cells in patients with differing coronary collateral support. *Circulation* 109:2986–92

Majka M, Janowska-Wieczorek A, Ratajczak J, Ehrenman K, Pietrzkowski Z, Kowalska MA, Gewirtz AM, Emerson SG, Ratajczak MZ (2001) Numerous growth factors, cytokines, and chemokines are secreted by human CD34(+) cells, myeloblasts, erythroblasts, and megakaryoblasts and regulate normal hematopoiesis in an autocrine/paracrine manner. *Blood* 97:3075–85

Natori Y, Ikezaki K, Matsushima T, Fukui M (1997) 'Angiographic moyamoya' its definition, classification, and therapy. *Clin Neurol Neurosurg* 99(Suppl 2): S168–72

Taguchi A, Matsuyama T, Moriwaki H, Hayashi T, Hayashida K, Nagatsuka K, Todo K, Mori K, Stern DM, Soma T, Naritomi H (2004*a*) Circulating CD34-positive cells provide an index of cerebrovascular function. *Circulation* 109:2972–5

Taguchi A, Matsuyama T, Nakagomi T, Shimizu Y, Fukunaga R, Tatsumi Y, Yoshikawa H, Kikuchi-Taura A, Soma T, Moriwaki H, Nagatsuka K, Stern DM, Naritomi H (2007) Circulating CD34-positive cells provide a marker of vascular risk associated with cognitive impairment. *J Cereb Blood Flow Metab*; e-pub ahead of print 8 August 2007

Taguchi A, Ohtani M, Soma T, Watanabe M, Kinosita N (2003) Therapeutic angiogenesis by autologous bone-marrow transplantation in a general hospital setting. *Eur J Vasc Endovasc Surg* 25:276–8

Taguchi A, Soma T, Tanaka H, Kanda T, Nishimura H, Yoshikawa H, Tsukamoto Y, Iso H, Fujimori Y, Stern DM, Naritomi H, Matsuyama T (2004*b*) Administration of CD34+ cells after stroke enhances neurogenesis via angiogenesis in a mouse model. *J Clin Invest* 114:330–8

ORIGINAL RESEARCH

Association between Signal Hyperintensity on T1-Weighted MR Imaging of Carotid Plaques and Ipsilateral Ischemic Events

N. Yamada
M. Higashi
R. Otsubo
T. Sakuma
N. Oyama
R. Tanaka
K. Iihara
H. Naritomi
K. Minematsu
H. Naito

BACKGROUND AND PURPOSE: To investigate associations between cerebral ischemic events and signal hyperintensity in T1-weighted MR imaging (T1WI) of carotid plaque according to stenosis severity and to estimate persistence of T1WI signal hyperintensity.

METHODS: A total of 222 patients (392 atherosclerotic carotid arteries) underwent plaque imaging using 3D inversion-recovery-based T1WI (magnetization-prepared rapid acquisition with gradient-echo [MPRAGE]). Carotid plaque with intensity on MPRAGE of >200% that of adjacent muscle was categorized as "high signal intensity" and correlated with ipsilateral ischemic events within the previous 6 months. A total of 58 arteries (35 patients) underwent repeat MR imaging a total of 70 times at a median interval of 279 days (range, 10–1037 days).

RESULTS: Ipsilateral ischemic events were more frequent in patients with MPRAGE high signals than in patients with low signals in the 0%–29%, 30%–69%, and 70%–99% stenosis groups: Relative risk (95% confidence interval) was 2.50 (0.96–6.51), 7.55 (1.84–31.04), and 1.98 (1.01–3.90), respectively. In the 70 cases of repeat MR imaging, 29 of 30 cases with high signals on the preceding MR imaging maintained high signals. Of the 58 arteries that underwent repeat MR imaging, 4 of 22 carotid arteries with high signals developed ipsilateral subsequent ischemic events within 1 year, whereas none with low signals developed subsequent events.

CONCLUSIONS: Carotid plaque signal hyperintensity on T1WI is strongly associated with previous ipsilateral ischemic events, persisting over a period of months, and may indicate risk of subsequent events. Larger clinical trials are warranted to clarify associations between signal hyperintensity and risk of subsequent cerebral ischemic events.

Atherosclerotic carotid plaque represents a major cause of cerebral ischemia.[1] Superiority of carotid endarterectomy to medical treatment has been confirmed for symptomatic carotid artery with severe stenosis (70%–99%) by the North American Symptomatic Carotid Endarterectomy Trial (NASCET) and the European Carotid Surgery Trial (ECST), but ≥7 operations were performed to avoid 1 stroke.[2,3] At the same time, symptomatic patients with 50%–69% stenosis have been shown to benefit from moderate reduction of stroke risk by surgery, whereas patients with <50% stenosis do not benefit from surgery.[2,3] However, cerebral ischemic episodes are not restricted to severe stenosis of the carotid artery,[2-4] and a substantial fraction of ischemic strokes in the territory of the carotid artery are unrelated to carotid stenosis.[1] Methods of noninvasively identifying "at risk" plaques are thus required.

Many studies have focused on MR imaging to characterize carotid plaques by using various imaging sequences. However, standardized sequence parameters and evaluation criteria to identify "at risk" plaques in MR imaging have not yet been established. Signal hyperintensity of carotid plaque in inversion recovery-based 3D T1-weighted imaging (alternatively known as magnetization-prepared rapid acquisition with gradient echo [MPRAGE])[5] was associated with recent ischemic events,[6,7] and was related to complicated plaques (type VI as proposed by the American Heart Association).[8,9]

We have performed carotid plaque imaging using MPRAGE since December 2001 for patients with suspected or confirmed carotid artery stenosis. The present study investigated associations between ischemic events and MPRAGE signal hyperintensity according to severity of stenosis in the carotid artery, and estimated persistence of MPRAGE signal hyperintensity as a potential risk factor for ischemic events.

Received December 17, 2005; accepted after revision April 11, 2006.

From the Department of Radiology (N.Y., M.H., T.S., R.T., H.N.), Cerebrovascular Division, Department of Medicine (R.O., N.O., K.M., H.N.), and Department of Neurosurgery (K.I.), National Cardiovascular Center, Osaka, Japan.

This study was supported by funding from the Japanese Ministry of Health, Labour, and Welfare.

Address correspondence to Naoaki Yamada, MD, Department of Radiology, National Cardiovascular Center, 5-7-1, Fujishirodai, Suita, Osaka, 565-8565 Japan; e-mail: naoyamad@hsp.ncvc.go.jp

Methods

Population

Since December 2001, MR imaging of the carotid artery has been performed for patients with suspected or confirmed atherosclerosis of the carotid artery after provision of oral informed consent on admission to the Departments of Neurology or Neurosurgery of our hospital. We reviewed the medical records of 222 consecutive patients who underwent MR imaging between December 2001 and June 2004. This study was performed in accordance with the ethics guidelines of our hospital. Of the 444 carotid arteries, 45 occluded arteries (at origin of the internal carotid artery, $n = 39$; common carotid artery, $n = 1$; top of the internal carotid artery or horizontal portion of the middle cerebral artery, $n = 5$) and 7 surgically treated carotid arteries (endarterectomy, $n = 5$; stent grafting, $n = 2$) were excluded from the study. A total of 392 carotid arteries from 222 patients were thus enrolled in this study.

Patient characteristics were recorded retrospectively by reviewing medical records. Ischemic events ipsilateral to the carotid artery within the previous 6 months were recorded, including cerebral infarction, transient ischemic attack, and retinal ischemia (amaurosis fugax and retinal artery occlusion). Emboligenic cardiac diseases (including persistent and paroxysmal atrial fibrillation, mitral valve stenosis, implantation of pros-

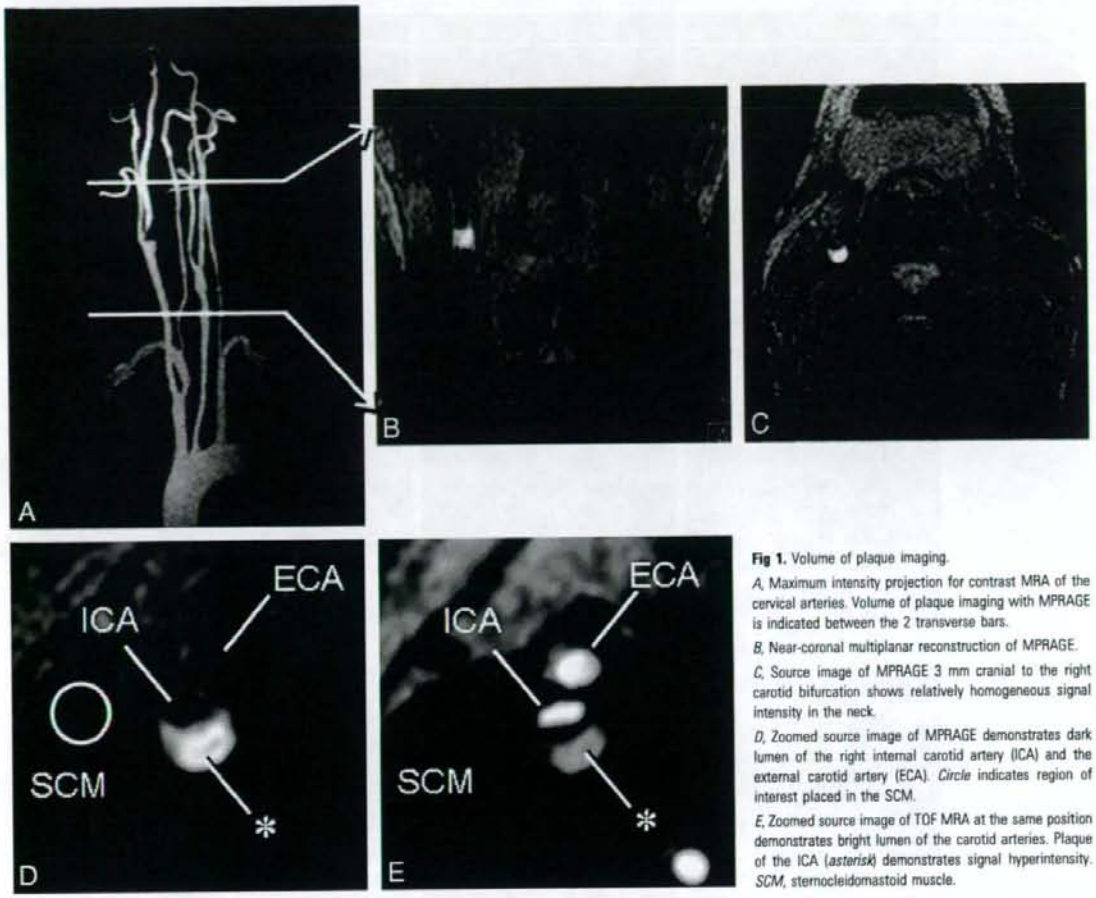

Fig 1. Volume of plaque imaging.

A, Maximum intensity projection for contrast MRA of the cervical arteries. Volume of plaque imaging with MPRAGE is indicated between the 2 transverse bars.

B, Near-coronal multiplanar reconstruction of MPRAGE.

C, Source image of MPRAGE 3 mm cranial to the right carotid bifurcation shows relatively homogeneous signal intensity in the neck.

D, Zoomed source image of MPRAGE demonstrates dark lumen of the right internal carotid artery (ICA) and the external carotid artery (ECA). *Circle* indicates region of interest placed in the SCM.

E, Zoomed source image of TOF MRA at the same position demonstrates bright lumen of the carotid arteries. Plaque of the ICA (*asterisk*) demonstrates signal hyperintensity. *SCM*, sternocleidomastoid muscle.

thetic heart valves, dilated cardiomyopathy, endocarditis, and acute myocardial infarction within the previous 6 months) were also recorded. Recorded risk factors of atherosclerosis included hypertension, diabetes mellitus, hyperlipidemia, and cigarette smoking.

MR Imaging

MR imaging was performed using a Magnetom Sonata 1.5T system (Siemens, Erlangen, Germany) with standard neck array and spine array coils (Fig 1). Plaque imaging was performed using MPRAGE in transaxial section with null blood condition (effective inversion time, 660 ms; TR, 1500 ms) and the water excitation technique to suppress fat signals. TR was defined as the interval between successive inversion pulses. Other imaging variables were: TE, 5.0 ms; FOV, 180 × 180 mm; matrix, 256 × 204; section thickness, 1.25 mm; 56 partitions; covering 70 mm around the carotid bifurcation; data acquisition time, 5 minutes. Multislab 3D time-of-flight (TOF) MR angiography (MRA) was also performed to facilitate delineation of lumen shape and plaque morphology (TE, 4.4 ms; TR, 35 ms; same spatial resolution as MPRAGE). Contrast MRA was performed after MPRAGE and 3D TOF MRA using rapid infusion of 0.1 mmol/kg body-weight gadolinium-diethylene-triaminepentaacetic acid (Gd-DTPA) at a rate of 2.0–3.0 mL/s after a test bolus of 1 mL Gd-DTPA for timing evaluation at the same rate. Typical imaging variables comprised: TR, 3.2 ms; TE, 1.3 ms; section thickness, 1.0 mm; 64 partitions; FOV, 360 × 200 mm; matrix, 512 × 208; data acquisition time, 14 seconds; near coronal section.

Follow-Up MR Imaging

Of the 222 patients, 28 patients underwent one repeat MR imaging and 7 patients underwent 2 repeat MRIs for follow-up of carotid atherosclerosis up to June 2005, depending on clinical demands. Among the 28 patients with one repeat MR imaging, 4 carotid arteries were excluded because of occlusion and 6 arteries were excluded as a result of surgical treatment before initial MR imaging ($n = 1$) and between initial and repeat MR imaging ($n = 5$). Among the 7 patients with 2 repeat MRIs, 2 arteries were excluded because of occlusion. MPRAGE signals from plaques were thus compared a total of 70 times in 58 arteries from 35 patients. For arteries that underwent 2 repeat MRIs, first repeat MR imaging was compared with initial MR imaging, and the second repeat MR imaging was compared with the first repeat MR imaging.

Evaluation of MR Imaging

Carotid stenosis was measured using contrast MRA according to the methods defined by the NASCET[10] and categorized into 3 groups: mild or no stenosis (0%–29%), moderate stenosis (30%–69%), and severe stenosis (70%–99%). One observer evaluated signal intensity of plaques on MPRAGE relative to signal intensity in adjacent muscle

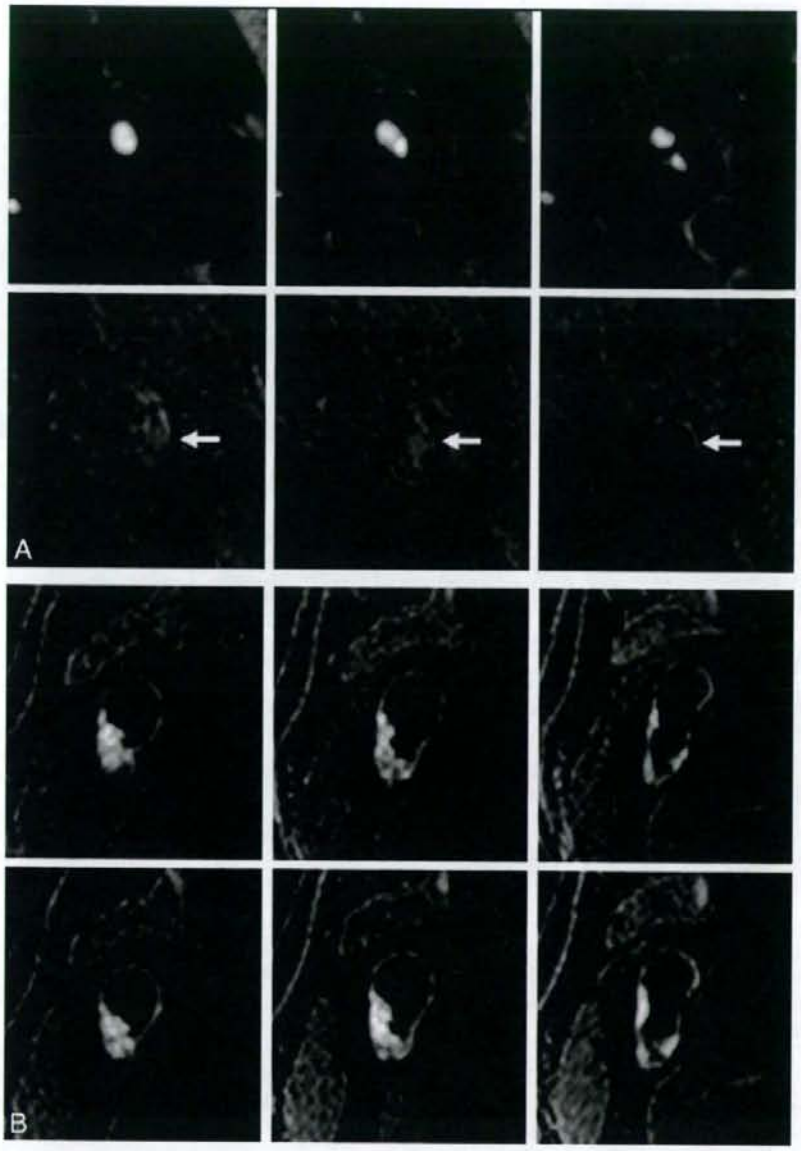

Fig 2. Examples of classic carotid plaques.

A, An example of low signal intensity plaque. Top and bottom rows show 3 corresponding sections with 2.5-mm intervals of TOF MRA and MPRAGE, respectively. A 76-year-old man has left carotid artery stenosis and no history of ipsilateral ischemic events. The carotid plaque (*arrows*) displays no signal hyperintensity relative to the adjacent muscle.

B, An example of high signal intensity plaque. Top and bottom rows show 3 corresponding sections with 2.5-mm intervals in initial and follow-up MR imaging. A 58-year-old man experienced cerebral infarction in the territory of the right middle cerebral artery 12 days before initial MR imaging, which reveals a right carotid plaque with heterogeneous MPRAGE signal hyperintensity (top row). At 4 months after initial MR imaging, the patient again developed cerebral infarction in the right middle cerebral artery territory. Follow-up MR imaging at 5 months after initial MR imaging (bottom row) shows mild increase of MPRAGE high signal intensity region.

(typically the sternocleidomastoid muscle) as measured by placing a round region of interest 5–8 mm in diameter on a standard console of the clinical MR system (Fig 1*D*). If the plaque displayed signal intensity >200% of muscle intensity at any place or section in the plaque, that plaque was categorized as "high signal intensity." Otherwise, the plaque was categorized as "low signal intensity" (Fig 2).

For carotid plaque with high signal intensity, volume of the region with signal intensity >200% of the muscle intensity was calculated using Dr. View/PRO version 5.2 software (Asahi Kasei Information Systems, Tokyo, Japan) on a stand-alone workstation.

Statistical Analysis

Two-tailed *t* tests or Mann-Whitney tests were used for comparison of means, 2-sided Fisher exact tests for comparison of proportions, paired *t* tests for comparison of paired variables, and χ^2 tests for linear trends of ischemic events according to stenosis severity. Associations

Table 1: Baseline characteristics of carotid arteries according to symptoms

	Symptomatic (n = 74)	Asymptomatic (n = 318)	P
Age (years)	69.9 ± 8.3*	70.0 ± 7.6	.8872
Female sex	14.9 (11/74)	17.3 (55/318)	.7309
AF and prosthetic heart valve	5.4 (4/74)	6.9 (22/318)	.7982
Hypertension	79.7 (59/74)	83.3 (265/318)	.4957
Diabetes mellitus	39.2 (29/74)	39.9 (127/318)	1.0000
Hyperlipidemia	62.2 (46/74)	56.0 (178/318)	.3630
Cigarette smoking	29.7 (22/74)	23.3 (74/318)	.2930

Note:—AF indicates atrial fibrillation. Values for age represent mean ± SD; other values represent percentage of carotid arteries, with raw numbers provided in parentheses.

between MPRAGE signal intensity and ipsilateral ischemic events were analyzed by considering each artery independently. All analyses were performed using Prism version 4.0 software for Windows (GraphPad Software, San Diego, Calif).

To calculate interobserver variability in categorization of carotid plaque as high or low signal intensity, a second observer categorized carotid plaque signals for the first 100 arteries after completing consensus reading of the last 10 carotid plaques as training between first and second observers. For calculation of intraobserver variability, the first observer repeated categorization of plaque signals for the first 100 arteries at >1 month after first observation. All interpretations of MR imaging were performed in a blinded manner. Interobserver and intraobserver agreement was calculated using κ statistics.

Results

Association between Signal Hyperintensity and Previous Ischemic Events

A total of 74 carotid arteries were associated with ipsilateral ischemic events within the previous 6 months (cerebral infarctions, $n = 45$; transient ischemic attack, $n = 20$; retinal ischemia, $n = 9$). Patients displaying carotid arteries with and without ipsilateral ischemic events exhibited no significant differences in age, sex, hypertension, diabetes mellitus, hyperlipidemia, or cigarette smoking status. A total of 24 carotid arteries were present in patients with atrial fibrillation, whereas 2 carotid arteries were from a single patient with a prosthetic aortic valve (Table 1). No patients were diagnosed with mitral stenosis, dilated cardiomyopathy, endocarditis, or acute myocardial infarction.

MPRAGE high signal intensity was assigned to 170 of 392 carotid plaques (Fig 2). The κ values for interobserver and intraobserver agreement were 0.729 and 0.792, respectively (good agreement). After excluding carotid arteries from patients with atrial fibrillation or prosthetic heart valves, a total of 370 carotid arteries were included in evaluation of association with previous ischemic events. Relative risks (95% confidence interval) of carotid arteries with MPRAGE high signals compared with carotid arteries with MPRAGE low signals for 0%–29%, 30%–69%, 70%–99% stenosis groups were 2.50 (0.96–6.51), 7.55 (1.84–31.04), and 1.98 (1.01–3.90), respectively (Table 2). In addition, risk of high signal intensity carotid arteries with 0%–29% and 30%–69% stenoses resembled risk of low signal intensity carotid arteries with 70%–99% stenosis: relative risks (95% confidence intervals [CI]) were 0.87 (0.34–2.24) and 1.34 (0.65–2.78), respectively. Frequency of ischemic events in MPRAGE high signal intensity plaques increased with stenosis severity ($P = .0133$). Median interval between MR imaging and previous ischemic events for MPRAGE high and low signal intensity groups was 20 days (range, 0–180 days) and 51 days (range, 6–179 days), respectively. Mann-Whitney tests revealed no significant differences between the 2 intervals ($P = .0854$).

In MRPAGE high signal intensity plaques, volume of the high signal intensity region was larger in symptomatic plaques than in asymptomatic plaques. Mean (± SD) volume for 0%–29%, 30%–69%, and 70%–99% stenosis groups in symptomatic plaques was 249 ± 301, 186 ± 327, and 166 ± 331 mm^3, respectively—larger than in asymptomatic plaques at 48 ± 72, 123 ± 169, and 115 ± 200 mm^3, respectively. Mann-Whitney tests revealed a significant difference for 0%–29% stenosis ($P = .0247$) but not for 30%–69% ($P = .5102$) or 70%–99% stenosis ($P = .3177$).

Follow-Up MR Imaging

A total of 70 comparisons in 58 arteries were performed between successive MRIs at a median interval of 279 days (range, 10–1037 days). Initial status of high or low signal intensity was maintained on repeat MR imaging for most comparisons; only 4 of 40 low signal intensity carotid arteries changed to high signal intensity, and only 1 of 30 high signal intensity carotid arteries changed to low signal intensity (Table 3). Volume of the region with signal intensity >200% of muscle intensity tended to be similar between successive MRIs ($P = .690$) (Fig 3). Mean stenosis did not change significantly in the 70 comparisons, at 44.2 ± 30.0% for the preceding MR imaging and 45.0 ± 30.2% for follow-up MR imaging ($P = .487$).

For investigation of subsequent events, 6 arteries from patients with atrial fibrillation and 2 arteries with ipsilateral middle cerebral artery occlusion at the horizontal portion were excluded from the 58 arteries. Among the remaining 50 carotid arteries, 4 of 22 carotid arteries with high signals displayed subsequent events, compared with 0 of 28 arteries with low signals ($P = .0473$) (Table 4). Repeat MR imaging of the 4 carotid arteries with subsequent events was performed at 9, 16, 16, and 27 days after subsequent events. Volume of the 4 arteries did not reveal any specific features compared with the other arteries (Fig 3).

Discussion

More ischemic events occurred in patients with high signals on MPRAGE than in those who showed low signals in each of the subgroups of patients with mild, moderate, and severe stenosis. Volume of high signal intensity was significantly larger in symptomatic plaque than in asymptomatic plaque for patients with mild stenosis. We also demonstrated in a subgroup that underwent multiple MR imaging that hyperintensity was maintained over a period of months, and MPRAGE high signals may offer an indicator of risk for subsequent events.

MPRAGE is a T1WI and displays intraplaque components that have short T1 as high signal intensity. Mechanisms of the short T1, however, are complex. Many previous studies have shown that lipid-rich necrotic cores display signal hyperintensity on T1WI.[11-14] Other studies have shown that intraplaque hemorrhage or thrombus exhibit high signal intensity on T1WI.[9,14-16] Although methemoglobin is considered to be a cause of high signal intensity, the duration of methemoglobin in carotid plaques remains unclear. Lipid signals are very weak in advanced plaques.[11] Signal hyperintensity in this study was not attributable to lipids, as fat-suppression technique was

Table 2: Risk of ipsilateral ischemia according to MPRAGE signal intensity and stenosis after excluding patients with atrial fibrillation and prosthetic heart valves

	0%–29% (n = 152)			30%–69% (n = 114)			70%–99% (n = 100)			Total (n = 366)		
Stenosis	S	A	F (%)	S	A	F (%)	S	A	F (%)	S	A	F (%)
MPRAGE												
High signal intensity	6	26	18.8	18	44	29.0	27	36	42.9	51	106	32.5
Low signal intensity	9	111	7.5	2	50	3.8	8	29	21.6	19	190	9.1
P		0.0889			0.0004			0.0498			<0.0001	
Relative risk (95% CI)		2.500 (0.9603–6.508)			7.548 (1.836–31.041)			1.982 (1.008–3.900)			3.573 (2.201–5.801)	

Note:—MPRAGE indicates magnetization-prepared rapid acquisition with gradient echo; S, symptomatic within previous 6 months; A, asymptomatic within previous 6 months; F, frequency of carotid arteries in patients with ipsilateral symptom; CI, confidence interval. P values were calculated using the Fisher exact test between MPRAGE high and low groups for symptoms (S) in each stenosis group. Relative risk of ischemic events was calculated for MPRAGE high carotid arteries compared with low carotid arteries in each stenosis group.

Table 3: Number of carotid arteries displaying MPRAGE high and low signal intensity according to interval between repeat and the preceding MRI, and signal intensity change on repeat MRI

	Number on Preceding MRI		Number Associated with Signal Intensity Change on Repeat MRI	
Interval	High	Low	High to Low	Low to High
<90 days	5	9	1	0
90–179 days	8	7	0	1
180–364 days	9	8	0	0
≥ 365 days	8	16	0	3
Total	30	40	1	4

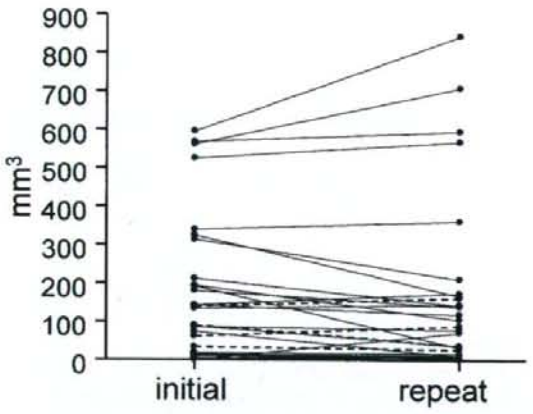

Fig 3. Comparison of high signal intensity volume between successive MR imaging. Comparison was done 34 times between 2 successive MR imagings with high signal intensity in both or either of the 2 MR images. Median interval was 279 days (range, 10–1037 days). High signal intensity volume (mean ± SD) was 149 ± 182 mm^3 at the initial MR imaging and 144 ± 217 mm^3 at the repeat MR imaging. Paired t test displayed no significant change (P = .690). Broken lines indicate 4 carotid arteries associated with subsequent events within 1 year after initial MR imaging.

used. Protein-rich viscous tissue can form another cause of signal hyperintensity.[17-19] The actual cause of T1WI signal hyperintensity should thus be investigated further.

In the follow-up study, signal hyperintensity was repeatedly observed (Table 3), and high signal intensity volume did not change significantly. Repeat MR imaging of 4 carotid arteries with subsequent events that was performed 9–27 days after these events exhibited no specific change in volume compared with the other arteries (Fig 3). These results may be attributable to continuous or recurrent intraplaque hemorrhage. However, we cannot conclude that signal hyperintensity is due to recent hemorrhage in this study. Erythrocyte membranes and iron have been shown to be present within the necrotic cores of human atherosclerotic coronary plaques even in the absence of recent hemorrhage, and intraplaque hemorrhage is related to progression and instability of such lesions.[20] If this is the case in carotid plaque, as in coronary plaque, the necrotic core of a carotid plaque can be at least partially formed by intraplaque hemorrhage, and thus no clear border would exist between intraplaque hemorrhage and necrotic core.

Size and location of high signals may be important for vulnerability. In the coronary artery, "at risk" plaques can be morphologically characterized by a large lipid-rich core and thin fibrous cap.[8,21] In the case of the carotid artery, however, numerous authors have stressed the importance of intraplaque hemorrhage.[22,23] Conversely, other authors have reported no significant differences in frequency of hemorrhage between symptomatic and asymptomatic patients.[24-26] The real causes of carotid plaque vulnerability thus remain controversial. Volume of the high signal intensity region was significantly larger in symptomatic carotid plaque than in asymptomatic plaque for the 0%–29% stenosis category, but not for the 30%–69% or 70%–99% categories. Carotid plaques with subsequent events did not display extremely large volumes for high signal intensity regions (Fig 3). Assessment of fibrous cap thickness and integrity is also important when evaluating plaque vulnerability and has been achieved using T2-weighted imaging and TOF MRA.[11,27,28] Some authors have reported higher percentages of symptomatic patients for ruptured caps (70%) compared with thick caps (9%) using multicontrast MR imaging.[29] Plaque ulceration may be related to stroke risk.[30,31] Better prediction of vulnerability may be achieved by combining MPRAGE with these techniques.

This study was performed using a commercially available clinical machine and standard neck- and spine-array coils without additional hardware. Image acquisition time was short (5 minutes for MPRAGE). MPRAGE with fat suppression and null blood condition suppresses background signals and highlights signal hyperintense tissues with short T1, so image interpretation is relatively simple.[7,9,32] Although motion artifacts were present to various degrees, predominantly attributable to respiration and swallowing, these were insufficient to result in the exclusion of any patients from the present study. 3D data acquisition is essential for visualizing the entirety of irregularly shaped plaques.

This study examined suspected and confirmed atherosclerotic carotid stenosis that may be related to cerebral ischemia depending upon clinical demands. Some biases in the study population

Table 4: Subsequent ipsilateral events according to stenosis severity and MPRAGE signals: results of 1 year follow-up after initial MRI

Stenosis	Number at Initial MRI	Subsequent Events		
		Ischemic Events	Surgical Treatment	Censored
Number of low signal intensity carotid arteries				
0%–29% Stenosis	9	0	0	1
30%–69% Stenosis	13	0	0	0
70%–99% Stenosis	6	0	3	0
Total	28	0	3	1
Number of high signal intensity carotid arteries				
0%–29% Stenosis	6	0	0	0
30%–69% Stenosis	7	1	1	0
70%–99% Stenosis	9	3	5	0
Total	22	4	6	0

Note:—MPRAGE indicates magnetization-prepared rapid acquisition with gradient echo. Ischemic events include ischemic stroke and transient ischemic attack. Surgical treatment includes carotid endarterectomy and endovascular stenting.

may thus be present. Reasons for MR imaging of the carotid artery varied, including screening of cervical artery stenosis, suspicion of complicated plaque on ultrasonography, inconclusive ultrasonography results due to calcification and high position of stenosis, refusal of conventional angiography by patients, and preoperative evaluation of carotid artery stenosis. Potential embolic sources, such as complicated plaque in the aortic arch and persistent foramen ovale, were not surveyed.

Conclusion

We conclude that carotid plaque hyperintensity on MPRAGE, a heavy 3D T1WI technique, is associated with previous cerebral ischemic events. MPRAGE hyperintense signals persist over a period of months, and may represent a potential indicator of risk for subsequent cerebral ischemia. Longitudinal studies with large subject populations are required to clarify whether MPRAGE hyperintense signals indicate risk of subsequent cerebral ischemic events.

Acknowledgments

We thank Teruo Noguchi from the National Cardiovascular Center for his helpful comments and discussions.

References

1. Barnett HJ, Gunton RW, Eliasziw M, et al. **Causes and severity of ischemic stroke in patients with internal carotid artery stenosis.** *JAMA* 2000;283:1429–36
2. Barnett HJ, Taylor DW, Eliasziw M, et al. **Benefit of carotid endarterectomy in patients with symptomatic moderate or severe stenosis. North American Symptomatic Carotid Endarterectomy Trial Collaborators.** *N Engl J Med* 1998;339:1415–25
3. Rothwell PM, Gutnikov SA,Warlow CP. **Reanalysis of the final results of the European Carotid Surgery Trial.** *Stroke* 2003;34:514–23
4. Golledge J, Greenhalgh RM, Davies AH. **The symptomatic carotid plaque.** *Stroke* 2000;31:774–81
5. Mugler JP 3rd, Brookeman JR. **Three-dimensional magnetization-prepared rapid gradient-echo imaging (3D MP RAGE).** *Magn Reson Med* 1990;15:152–57
6. Moody AR, Allder S, Lennox G, et al. **Direct magnetic resonance imaging of carotid artery thrombus in acute stroke.** *Lancet* 1999;353:122–23
7. Murphy RE, Moody AR, Morgan PS, et al. **Prevalence of complicated carotid atheroma as detected by magnetic resonance direct thrombus imaging in patients with suspected carotid artery stenosis and previous acute cerebral ischemia.** *Circulation* 2003;107:3053–58
8. Stary HC, Chandler AB, Dinsmore RE, et al. **A definition of advanced types of atherosclerotic lesions and a histological classification of atherosclerosis. A report from the Committee on Vascular Lesions of the Council on Arteriosclerosis, American Heart Association.** *Arterioscler Thromb Vasc Biol* 1995;15:1512–31
9. Moody AR, Murphy RE, Morgan PS, et al. **Characterization of complicated carotid plaque with magnetic resonance direct thrombus imaging in patients with cerebral ischemia.** *Circulation* 2003;107:3047–52
10. Anonymous. **North American Symptomatic Carotid Endarterectomy Trial. Methods, patient characteristics, and progress.** *Stroke* 1991;22:711–20
11. Toussaint JF, Southern JF, Fuster V, et al. **T2-weighted contrast for NMR characterization of human atherosclerosis.** *Arterioscler Thromb Vasc Biol* 1995;15:1533–42
12. Rogers WJ, Prichard JW, Hu YL, et al. **Characterization of signal properties in atherosclerotic plaque components by intravascular MRI.** *Arterioscler Thromb Vasc Biol* 2000;20:1824–30
13. Yuan C, Kerwin WS, Ferguson MS, et al. **Contrast-enhanced high resolution MRI for atherosclerotic carotid artery tissue characterization.** *J Magn Reson Imaging* 2002;15:62–67
14. Yuan C, Mitsumori LM, Ferguson MS, et al. **In vivo accuracy of multispectral magnetic resonance imaging for identifying lipid-rich necrotic cores and intraplaque hemorrhage in advanced human carotid plaques.** *Circulation* 2001;104:2051–56
15. Cappendijk VC, Cleutjens KB, Heeneman S, et al. **In vivo detection of hemorrhage in human atherosclerotic plaques with magnetic resonance imaging.** *J Magn Reson Imaging* 2004;20:105–10
16. Cappendijk VC, Cleutjens KB, Kessels AG, et al. **Assessment of human atherosclerotic carotid plaque components with multisequence MR imaging: initial experience.** *Radiology* 2005;234:487–92
17. Hayashi Y, Tachibana O, Muramatsu N, et al. **Rathke cleft cyst: MR and biomedical analysis of cyst content.** *J Comput Assist Tomogr* 1999;23:34–38
18. Ahmadi J, Destian S, Apuzzo ML, et al. **Cystic fluid in craniopharyngiomas: MR imaging and quantitative analysis.** *Radiology* 1992;182:783–85
19. Kucharczyk W, Macdonald PM, Stanisz GJ, et al. **Relaxivity and magnetization transfer of white matter lipids at MR imaging: importance of cerebrosides and pH.** *Radiology* 1994;192:521–29
20. Kolodgie FD, Gold HK, Burke AP, et al. **Intraplaque hemorrhage and progression of coronary atheroma.** *N Engl J Med* 2003;349:2316–25
21. Libby P, Aikawa M. **Stabilization of atherosclerotic plaques: new mechanisms and clinical targets.** *Nat Med* 2002;8:1257–62
22. Lusby RJ, Ferrell LD, Ehrenfeld WK, et al. **Carotid plaque hemorrhage. Its role in production of cerebral ischemia.** *Arch Surg* 1982;117:1479–88
23. Imparato AM, Riles TS, Mintzer R, et al. **The importance of hemorrhage in the relationship between gross morphologic characteristics and cerebral symptoms in 376 carotid artery plaques.** *Ann Surg* 1983;197:195–203
24. Bassiouny HS, Davis H, Massawa N, et al. **Critical carotid stenoses: morphologic and chemical similarity between symptomatic and asymptomatic plaques.** *J Vasc Surg* 1989;9:202–12
25. Hatsukami TS, Ferguson MS, Beach KW, et al. **Carotid plaque morphology and clinical events.** *Stroke* 1997;28:95–100
26. Svindland A, Torvik A. **Atherosclerotic carotid disease in asymptomatic individuals: An histological study of 53 cases.** *Acta Neurol Scand* 1988;78:506–17
27. Toussaint JF, LaMuraglia GM, Southern JF, et al. **Magnetic resonance images lipid, fibrous, calcified, hemorrhagic, and thrombotic components of human atherosclerosis in vivo.** *Circulation* 1996;94:932–38
28. Hatsukami TS, Ross R, Polissar NL, et al. **Visualization of fibrous cap thickness and rupture in human atherosclerotic carotid plaque in vivo with high-resolution magnetic resonance imaging.** *Circulation* 2000;102:959–64
29. Yuan C, Zhang SX, Polissar NL, et al. **Identification of fibrous cap rupture with magnetic resonance imaging is highly associated with recent transient ischemic attack or stroke.** *Circulation* 2002;105:181–85
30. Eliasziw M, Streifler JY, Fox AJ, et al. **Significance of plaque ulceration in symptomatic patients with high-grade carotid stenosis. North American Symptomatic Carotid Endarterectomy Trial.** *Stroke* 1994;25:304–08
31. Rothwell PM, Gibson R, Warlow CP. **Interrelation between plaque surface morphology and degree of stenosis on carotid angiograms and the risk of ischemic stroke in patients with symptomatic carotid stenosis. On behalf of the European Carotid Surgery Trialists' Collaborative Group.** *Stroke* 2000;31:615–21
32. Moody AR, Pollock JG, O'Connor AR, et al. **Lower-limb deep venous thrombosis: direct MR imaging of the thrombus.** *Radiology* 1998;209:349–55

INTERNAL MEDICINE

□ CASE REPORT □

Paradoxical Cerebral Embolism Causing Internal Carotid Artery Occlusion

Shuhei Okazaki, Masahiro Oomura, Kuni Konaka, Atsuko Shimode and Hiroaki Naritomi

Abstract

Paradoxical cerebral embolism (PCE) is defined to be a pathological condition in which emboli originating from the venous system reach the cerebral arterial circulation via the right-to-left (R-L) shunt. In patients with PCE, emboli originating from the venous system most commonly pass through the patent foramen ovale during Valsalva-provoking activities which increase the right atrial pressure above the left atrial pressure. The size of cerebral infarction caused by PCE is generally small, since the size of emboli which can pass through the R-L shunt is small. Here, we report a case of PCE which occluded the internal carotid artery (ICA).

Key words: paradoxical embolism, internal carotid artery, pulmonary embolism, deep vein thrombosis

(DOI: 10.2169/internalmedicine.46.6046)

Case Report

A 64-year-old female was admitted to our hospital because of disturbed consciousness, hypoxemia and left hemiparesis. The patient had a history of insomnia, depression, and hyperlipidemia.

On admission, physical examination revealed a cyanotic woman with respiratory rate 18 times per minute. Her body temperature was 37.0℃, blood pressure 100/50 mmHg, and her heart rate was increased to 108 beats per minute. On neurological examination, she was lethargic. Her eyes were deviated to the right. She had left hemiparesis. The laboratory findings were as follows (normal values in bracket): serum levels of FDP and D-dimer were elevated to 25 μg/ml (<5 μg/ml) and 16.0 μg/ml (<1.0 μg/ml), respectively. The blood gas analysis disclosed severe hypoxemia with hypocapnia showing PaO_2 48 mmHg and $PaCO_2$ 28 mmHg. Carotid duplexsonography showed no atherosclerotic change in either side of carotid arteries. Diastolic flow velocity of right ICA was not detected by duplex scanning suggesting the distal occlusion of right ICA. Magnetic resonance (MR) imaging revealed acute infarction in the right basal ganglia (Fig. 1-A). MR angiography disclosed the occlusion of the right ICA (Fig. 1-B). The enhanced chest computed tomography revealed filling defects in both pulmonary arteries. Perfusion lung scintigraphy showed multiple perfusion defects in both sides of the lungs (Fig. 1-C). These findings were consistent with pulmonary thromboembolism. The pulmonary arterial pressure, estimated using transthoracic echocardiogram, was increased to approximately 80 mmHg. Transesophageal echocardiography (TEE) detected no thrombus in the left atrium or appendage, and no complicated atheroma in the aortic arch but demonstrated the R-L shunt through patent foramen ovale (PFO) definitively without Valsalva maneuver (Fig. 2). The contrast transcranial color-coded sonography (TCCS) also confirmed the R-L shunt without Valsalva maneuver. Duplexsonography of lower extremities revealed multiple thrombi in the right popliteal, posterior tibial, and peroneal deep veins. The diagnosis of PCE in association with pulmonary thromboembolism was established on the basis of clinical, laboratory, and radiological findings. She was treated conservatively with intravenous heparin administration followed by oral warfarin administration. Her right hemiparesis and hypoxemia were markedly improved to the degree that she could walk without aids in the room air. The contrast TCCS at one month after onset failed to demonstrate the R-L shunt even during Valsalva maneuver. The pulmonary arterial pressure was declined to approximately 46 mmHg at that time. She was discharged with minimal neurological deficits.

Department of Cerebrovascular Medicine, National Cardiovascular Center, Suita
Received for publication May 21, 2006; Accepted for publication October 1, 2006
Correspondence to Dr. Shuhei Okazaki, s-okazaki@umin.ac.jp